ELSEVIER

International Journal of Mass Spectrometry 201 (2000) 187–195

International Journal of Mass Spectrometry

Electron-impact total ionization cross sections of $SF_x(x = 1–5)$

M. Asgar Ali[a], Karl K. Irikura[b,*], Yong-Ki Kim[c]

[a]*Department of Chemistry, Howard University, Washington D.C. 20059, USA*
[b]*Physical and Chemical Properties Div. National Institute of Standards and Technology, Gaithersburg, Maryland 20899-8380, USA,*
[c]*Atomic Physics Div. National Institute of Standards and Technology, Gaithersburg, Maryland 20899-8423, USA*

Received 17 November 1999; accepted 10 December 1999

Abstract

Total cross sections for electron impact ionization are necessary quantities for numerical modeling of plasma chemistry and for quantitative mass-spectrometric gas analysis. Theoretical cross sections for SF, SF_2, SF_3, SF_4, and SF_5 are calculated by the recently developed binary-encounter-Bethe (BEB) model. The BEB model combines a modified form of the Mott cross section and the Bethe cross section. The results are compared with experimental cross sections for SF_3 and SF_5 free radicals. In view of the success of the BEB method for SF_6 and many other molecules, it is expected that the results presented here will provide reliable total ionization cross sections for $SF_x(x = 1–5)$. (Int J Mass Spectrom 201 (2000) 187–195) © 2000 Elsevier Science B.V.

Keywords: Electron impact ionization; Ionization cross section; Sulfur fluorides; SF_6; Theory

1. Introduction

Because of the widespread use of sulfur hexafluoride as an insulator in the power industry and for pulsed power generation and plasma processing, considerable experimental and theoretical studies [1] have been devoted to ion formation processes and breakdown phenomena in SF_6 and gas mixtures containing SF_6. Rapp and Englander-Golden [2] measured the total ionization cross section σ_i for SF_6 due to electron impact under controlled single collision conditions. Stanski and Adamzyk [3] and Märk and co-workers [4] determined partial ionization cross sections of SF_6. The total ionization cross section of SF_6 calculated by Kim and co-workers [5] using the binary-encounter–Bethe (BEB) model and by Deutsch et al. [6] using a modified additivity rule agree well with each other and with the experimental cross section by Rapp and Englander-Golden [2]. Recently Tarnovsky et al. [7] reported partial cross sections for the electron-impact ionization and dissociative ionization of SF_3 and SF_5 from threshold to 200 eV in incident electron energy. However, no experimental results are available for SF, SF_2, or SF_4. The molecular structures and thermochemistry of SF_x and SF_x^+ were determined from ab initio theory by Irikura [8] and subsequently refined by Bauschlicher and Ricca [9]. In the present article we report electron-impact total ionization cross sections for $SF_x(x = 1–5)$ calculated using the BEB model and compare them to available experimental and theoretical results.

There have been numerous efforts to combine the Mott cross section [10] with the Bethe theory [11]

* Corresponding author. karl.irikura@nist.gov

PII S1387-3806(00)00211-6

since the 1950s [12–16]. However, these attempts used semiempirical parameters specific to each target atom or molecule and were not easily extendable to large molecules or radicals with no experimental data for either the molecules themselves or the constituent atoms. Another semiempirical theory is Deutsch's and Märk's "DM formalism," which combines a classical binary-encounter theory with an additivity rule. In the DM formalism for molecules [17], semiempirical weights are introduced for each atomic orbital of the constituent atoms of a molecule, while additional molecular orbital factors are assigned using a Mulliken population analysis.

Kim and Rudd [18] developed a theory of σ_i for electron-impact ionization of molecules by combining a modified form of the Mott cross section at low incident electron energy T and the Bethe theory for high T. Unlike earlier attempts, the theory by Kim and Rudd does not involve empirical parameters specific to each target molecule. The simplest form for the cross section proposed by Kim and Rudd, the BEB model, uses theoretical (ab initio) data from the ground-state molecular wave function, except for the lowest ionization energy (IE), for which an experimental vertical IE, if available, is used to match the experimental threshold. If no experimental vertical IE is available, the value from an advanced ab initio calculation is used.

Kim and co-workers [5,19–23] have shown that molecular wave functions of modest accuracy (e.g. Hartree–Fock) can produce σ_i in good agreement (15% or better at the peak) with available experimental data from threshold to $T = 5$ keV for a wide range of molecules, such as H_2, SF_6, and C_3F_8. We expect the predictions for SF_x molecules to be equally reliable.

2. Theory

Kim and Rudd [18] proposed the binary encounter dipole (BED) model to calculate singly differential ionization cross sections (i.e. cross section as a function of the energy of the ejected electron) by using the differential form of the Mott theory [10] and the Bethe theory [11]. They also required the ionization cross section itself and the corresponding stopping cross section to satisfy the asymptotic behavior of the Bethe theory at high T. The stopping cross section is the integral of the product of the energy transfer from the incident electron to the target and the corresponding differential ionization cross section. The BED model requires explicit knowledge of the differential continuum dipole oscillator strength, $f(W)$, for each occupied molecular orbital in the initial state of the target molecule, where W is the energy of the ejected electron. The differential cross section is then integrated over W to obtain the total ionization cross section for each molecular orbital characterized by its binding energy B, average electron kinetic energy $U = \langle \mathbf{p}^2/2m_e \rangle$, and electron occupation number N.

The kinetic energy U for each orbital in the initial state (usually the ground state) of the target is a theoretical quantity evaluated by any atomic or molecular wave function code that calculates the total energy. However, both the initial- and continuum-state wave functions are needed for calculating $f(W)$. Although $f(W)$ can be deduced from experimental photoionization cross sections, it is difficult to deduce the individual contribution from each orbital. In principle one can calculate $f(W)$ for each orbital. In practice, however, it is feasible only for a limited number of atoms and very few molecules. To overcome this difficulty, Kim and Rudd [18] introduced a simplified version of the BED model, i.e. the BEB model, when no information on $f(W)$ was available. This simplification greatly extends the applicability of the method.

In the BEB model, a simple form for $f(w)$ ($w = W/B$) is used

$$f(w) = N/(w + 1)^2 \tag{1}$$

such that the integrated cross section σ_{BEB} per orbital is given by

$$\sigma_{\mathrm{BEB}} = \frac{S}{t + (u + 1)/n}\left[\frac{\ln t}{2}\left(1 - \frac{1}{t^2}\right) + 1 - \frac{1}{t} - \frac{\ln t}{t + 1}\right] \tag{2}$$

where $t = T/B$, $u = U/B$, $S = 4\pi a_0^2 N R^2/B^2$, a_0 is the Bohr radius, and R is the Rydberg energy.

The constant n in Eq. (2) is unity in most cases. However, when the molecular orbital is dominated by an atomic orbital with principal quantum number ≥ 3 (as judged by the Mulliken population being more than ~85%), then n equals the principal quantum number. This adjustment is ad hoc in nature, unlike the rest of Eq. (2), and is based in part on the observation that radial functions of atomic orbitals with high principal quantum numbers have high kinetic energies that reduce the orbital cross sections too much. The original form of the Mott and Bethe cross sections does not contain $u + 1$ in the denominator of Eq. (2). This factor was introduced to correct the tendency of most theories to overestimate cross sections at low T between the threshold and the peak. Since the original Mott formula is for a free target electron, the $u + 1$ factor should be reduced and eventually eliminated for loosely bound target electrons. The reduction of $u + 1$ for loosely bound electrons is also consistent with the observation that the orbital kinetic energies of nodeless valence orbitals obtained with pseudopotentials or effective potentials for the core are similar in magnitude as the recipe used above, viz. $(u + 1)/n$ [23].

Eq. (2) requires as input only B, U, and N for each molecular orbital in the ground state. These constants can be determined using a molecular wave function code. The total ionization cross section σ_i is then simply the sum of σ_{BEB} over all occupied molecular orbitals

$$\sigma_i = \sum_{\mathrm{MO}} \sigma_{\mathrm{BEB}} \tag{3}$$

3. Molecular wave functions

Based on applications to over 50 molecules [24], we found that σ_i is most sensitive to the lowest value of B. To match the experimental cross sections near the lowest ionization threshold, it is necessary to use a realistic vertical IE. Hence, we use the experimental value of the first ionization energy if a reliable value is available. Otherwise we use a theoretical value from a well-correlated ab initio calculation. All other parameters are determined using ab initio methods.

The actual values of the molecular constants needed depend on the level of approximation used for the target wave function. The self-consistent field method provides the simplest molecular wave function. The kinetic energy U is determined directly as an expectation value. To get B, one can use orbital energies as an approximation (Koopmans' theorem).

4. Details of molecular calculations [25]

Following our previous practice [18–22], we used the molecular structure code GAMESS [26] to calculate Hartree–Fock orbital binding energies B and orbital kinetic energies U (Table 1). Cartesian 6-311+G(d) basis sets, as implemented in GAMESS, were used for these calculations. Although experimental adiabatic IEs are known for these molecules, vertical IEs are not available. The vertical IEs were calculated previously [8] using the frozen-core quadratic configuration interaction QCISD(T) theory [27] and spherical 6-311G(d) basis sets. We have improved upon these somewhat by using the frozen-core coupled-cluster theory including all single and double substitutions and a perturbative estimate of connected triples (CCSD(T)) [28] together with the larger cc-pVTZ basis sets of Dunning and co-workers [29,30]. Binding and kinetic energies are insensitive to details of the molecular geometry. Thus, for convenience, we used HF/6-311+G(d) geometries for the GAMESS calculations and hybrid density functional B3LYP/6-31G(d) [31,32] geometries for the coupled-cluster calculations. These geometries are very similar to each other and to those previously published [8,9]. The ACES II program [33,34] suite was used for the coupled-cluster calculations and the GAUSSIAN 98 program [35] was used for the B3LYP calculations. We adopt the CCSD(T) vertical IEs here. They are summarized in Table 2 along with the earlier results [8]. All open-shell calculations (viz., SF, SF_3, and SF_5) were spin-unrestricted. For conciseness, the binding and kinetic energies for matching α and β orbitals were averaged to produce Table 1. We have found in the past [20], and have verified in the present cases,

Table 1
Binding energies (B), kinetic energies (U), and occupation numbers (N) for each molecular orbital (MO) in SF_x (x = 1–5). For open-shell molecules, the unrestricted Hartree-Fock results for matched α and β orbitals have been averaged together. The lowest value of B for each molecule is taken from Table 2

MO	B (eV)	U (eV)	N
SF $C_{\infty v}$ $^2\Pi$			
2σ	716.99	1013.49	2
3σ	246.84	509.35	2
1π	183.67	479.77	4
4σ	183.77	478.68	2
5σ	44.79	102.56	2
6σ	26.11	77.86	2
2π	19.50	80.86	4
7σ	18.38	75.71	2
3π	10.75	56.05	3
SF_2 C_{2v} $^1A_1$			
$1b_1$	717.08	1013.44	2
$2a_1$	717.08	1013.45	2
$3a_1$	247.70	509.31	2
$2b_1$	184.64	478.48	2
$4a_1$	184.58	478.96	2
$1b_2$	184.46	480.49	2
$5a_1$	45.92	98.57	2
$3b_1$	44.66	106.08	2
$6a_1$	27.03	84.14	2
$4b_1$	21.35	82.41	2
$7a_1$	20.72	75.54	2
$2b_2$	20.61	76.86	2
$1a_2$	19.31	86.94	2
$5b_1$	18.35	89.89	2
$8a_1$	16.53	78.18	2
$3b_2$	10.28	64.86	2
SF_3 C_s $^2A'$			
$2a'$	718.11	1013.47	2
$3a'$	716.22	1013.48	2
$1a''$	716.21	1013.49	2
$4a'$	250.84	510.27	2
$5a'$	187.88	479.27	2
$2a''$	187.73	478.44	2
$6a'$	187.37	478.83	2
$7a'$	47.20	97.14	2
$3a''$	44.13	103.14	2
$8a'$	43.97	105.87	2
$9a'$	28.43	88.56	2
$4a''$	22.61	79.32	2
$10a'$	22.01	76.19	2
$11a'$	21.31	77.66	2
$5a''$	20.24	82.54	2
$12a'$	18.77	84.29	2
$6a''$	18.44	84.68	2
$13a'$	18.08	87.23	2
$7a''$	17.75	90.34	2
$14a'$	14.69	84.10	2
$15a'$	11.08	81.36	1

Table 1
(Continued)

MO	B (eV)	U (eV)	N
SF_4 C_{2v} $^1A_1$			
$1b_2$	718.72	1013.45	2
$2a_1$	718.72	1013.45	2
$3a_1$	716.17	1013.45	2
$1b_1$	716.17	1013.45	2
$4a_1$	252.84	510.40	2
$2b_2$	189.72	478.55	2
$2b_1$	189.72	478.74	2
$5a_1$	189.62	479.44	2
$6a_1$	48.97	92.90	2
$3b_2$	46.94	105.15	2
$3b_1$	44.46	101.99	2
$7a_1$	43.96	107.55	2
$8a_1$	29.41	93.61	2
$4b_2$	23.97	83.24	2
$4b_1$	23.80	79.70	2
$9a_1$	23.37	73.23	2
$1a_2$	21.91	80.25	2
$5b_2$	20.25	90.00	2
$10a_1$	20.24	84.97	2
$5b_1$	20.13	83.48	2
$6b_2$	18.29	87.25	2
$11a_1$	18.29	87.40	2
$6b_1$	18.03	92.68	2
$2a_2$	17.84	93.16	2
$12a_1$	12.82	85.04	2
SF_5 C_{4v} $^2A_1$			
$2a_1$	718.64	1013.43	2
$1b_1$	717.67	1013.44	2
$1e$	717.67	1013.45	4
$3a_1$	717.67	1013.46	2
$4a_1$	254.41	510.35	2
$5a_1$	191.33	479.33	2
$2e$	191.42	478.95	4
$6a_1$	49.60	89.33	2
$3e$	46.15	102.32	4
$7a_1$	46.20	105.80	2
$2b_1$	44.82	110.03	2
$8a_1$	29.91	96.00	2
$4e$	24.73	81.05	4
$9a_1$	24.20	78.58	2
$1b_2$	22.17	76.03	2
$5e$	21.68	81.06	4
$3b_1$	20.01	88.13	2
$10a_1$	19.79	87.08	2
$4b_1$	19.04	87.96	2
$6e$	19.31	91.47	4
$7e$	19.05	93.02	4
$1a_2$	18.35	97.27	2
$11a_1$	11.70	92.80	1

Table 2
Vertical ionization energies (in eV) calculated at the QCISD(T)/6-311G(d) level [8] and at the CCSD(T)/cc-pVTZ level. Vibrational zero-point energies are ignored

Molecule	QCISD(T)	CCSD(T)
SF	10.24	10.15 ($^3\Sigma^-$)
		10.55 ($^1\Delta$)
		11.54 ($^1\Sigma^+$)
SF_2	10.36	10.28
SF_3	10.93	11.08
SF_4	12.83	12.82
SF_5	11.46	11.70

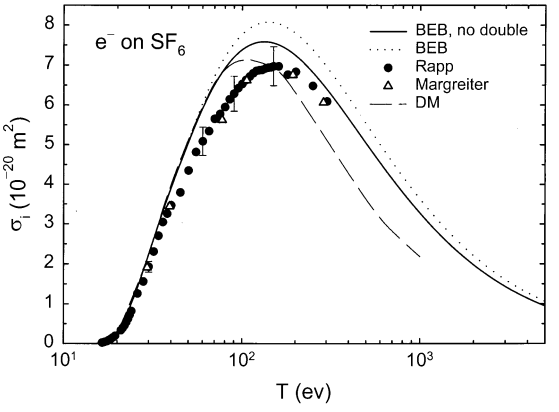

Fig. 1. Total ionization cross section for SF_6 under electron impact. Experimental data (filled circles) and uncertainties are from [2]. Open triangles indicate experimental measurements from [4], which were calibrated against those of [2] at $T = 100$ eV. The solid and dotted curves indicate the cross sections calculated using BEB theory. The dotted curve, which includes double ionization, should be compared with the experimental data. The dashed curve, taken from [37] was calculated using the alternative DM formalism.

that this averaging has a negligible effect on the computed cross sections.

In many experiments, collisions that produce doubly charged ions (or a pair of singly charged ions) are counted twice. We assumed that all holes generated in molecular orbitals with binding energies greater than the double-ionization threshold will decay through the Auger process, resulting in a doubly charged ion or two singly charged fragments. In either case we estimated the contribution of double ionization to the gross ionization cross section by doubling the BEB cross sections for the inner-shell orbitals. The thresholds were taken to be the adiabatic double ionization energies, that is, the energy difference between SF_x and SF_x^{++} at their respective geometries, using frozen-core CCSD(T)/cc-pVTZ//B3LYP/6-31G(d) calculations as before. No bound structure was found for SF_5^{++}, so the threshold was taken to be the sum of the adiabatic ionization energy of SF_5 (9.46 eV) and the vertical ionization energy of SF_5^+ (23.44 eV), calculated at the coupled-cluster level. The calculated threshold energies for the double ionization of SF_x were thus 31.08, 29.60, 29.78, 28.70, and 32.91 eV for $x = 1$–5, respectively.

SF_6 is included here to illustrate the agreement between the BEB theory and well-established experimental results. Orbital binding and kinetic energies were taken from an earlier publication by Hwang et al. [5], except that we adopted a vertical ionization energy of 15.65 eV computed using the coupled-cluster method (see above). Since not even the singly charged ion is covalently bound, we used a coupled-cluster value for the vertical double-ionization energy (38.03 eV) as the threshold for double ionization.

5. Results and discussion

As reported earlier [5,36], BEB cross sections for SF_6 agree well with the experimental measurements [2]. With the minor differences from [5] that were noted above, the comparison is shown in Fig. 1. Among the species SF_x ($x = 1$–5), experimental electron-impact ionization cross sections have been reported only for SF_5 and SF_3 [7]. We compare our BEB cross sections with experimental values for SF_5 and SF_3 in Figs. 2 and 3. Predictions of the modified additivity rule [6] are also drawn in the figures; these are taken from Fig. 4 of [7].

5.1. SF_6

The calculated cross section for SF_6 is in acceptable agreement with the experimental data [2,4]. The experimental peak is 7.0 ± 0.5 Å^2 at 155 eV incident energy [2], while the BEB peak is 8.1 Å^2 at 140 eV (the peak is 7.6 Å^2 at 133 eV if double ionization is

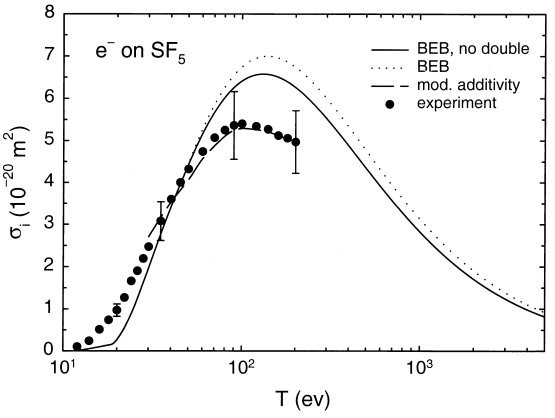

Fig. 2. Total ionization cross section for SF_5 under electron impact. Experimental data, uncertainties, and the dashed predictive curve are from [7]. The solid BEB curve, which excludes double ionization, should be compared with the experimental data.

excluded). Since total ion current was measured in the experiment, double ionization should be included. Thus, the calculated peak cross section exceeds the experimental value by (16 ± 8)% and is displaced by −15 eV. The BEB theory provides the total cross section for electronic excitation with the energy transfer to the target exceeding the lowest IE. The usual fate of the excited molecule is ionization, so the BEB cross section is identified with the ionization cross section. However, for larger molecules, some of the excitation energy may be transferred to vibrational motions of the molecule. This may lead to neutral fragmentation or, for very large molecules, to radiative or collisional relaxation. Thus, assuming that reasonable values for binding and kinetic energies are used, the BEB cross section is expected to exceed the ionization cross section by a margin that increases with molecular size. The contribution of nonionizing channels appears to be on the order of 15% for SF_6. Theoretical predictions from the DM formalism [37], also shown in Fig. 1, agree with the BEB predictions from threshold to about 100 eV.

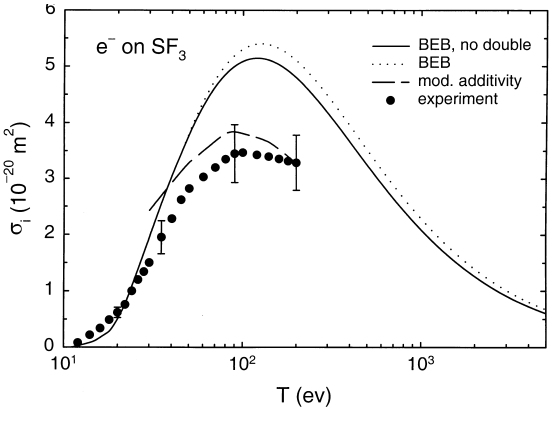

Fig. 3. Total ionization cross section for SF_3 under electron impact. Experimental data, uncertainties, and the dashed predictive curve are from [7]. The solid BEB curve, which excludes double ionization, should be compared with the experimental data.

5.2. SF_5

In contrast to the current-measuring experiments involving SF_6, the measurements of Tarnovsky et al. [7] for SF_5 and SF_3 included only mass-selected, singly charged ions. Doubly charged ions were thus excluded from the measured cross sections. Singly charged fragments may be produced from a doubly charged ion and be detected. However, the corresponding "Coulomb explosion" may produce fast ions, which are detected less efficiently [7]. Thus, we choose to compare the experimental cross sections with BEB calculations that exclude double ionization i.e. the counting ionization cross section. These are the solid curves in Figs. 1–6. The dotted curves are provided to indicate the expected contribution from double ionization.

The experimental cross section peak is 5.4 ± 0.8 Å^2, at $T \approx 100$ eV. The BEB peak is higher, 6.6 Å^2 at $T = 132$ eV. The discrepancy, (25 ± 19)% and 32 eV, is significantly larger than for SF_6. In the experimental study, only SF_5^+ and SF_4^+ were collected, with their abundance being found almost equal. No allowance was made in the experimental cross section for contributions from unobserved fragment ions (viz. SF_3^+, SF_2^+, SF^+, S^+, and F^+). An upper limit of the contributions from these lighter ions was estimated to be 0.25 Å^2 at 70 eV [7]. Including this would shift the experimental peak to somewhat higher energy and could bring the discrepancy in intensity as low as (19 ± 17)%.

The theoretical cross sections are substantially

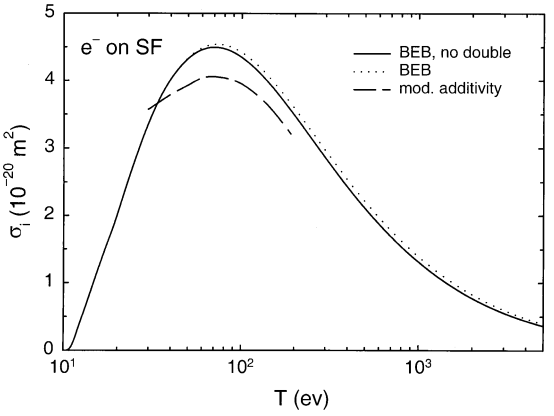

Fig. 4. Total ionization cross section for SF under electron impact. The dashed curve shows the predictions from the modified additivity rule [7]. The solid and dotted curves are the predictions from BEB theory.

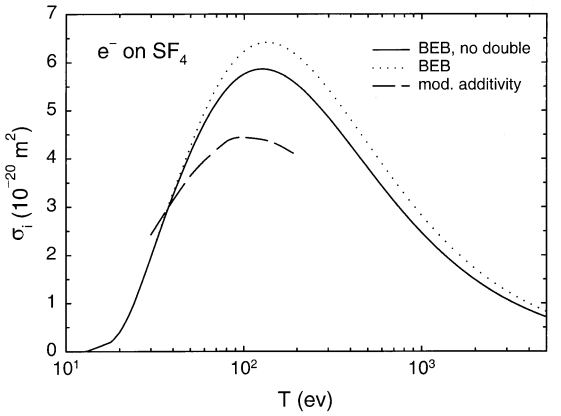

Fig. 6. Total ionization cross section for SF_4 under electron impact. The dashed curve shows the predictions from the modified additivity rule [7]. The solid and dotted curves are the predictions from the BEB theory.

lower than the measurements at low energies. As discussed above in the paragraph on SF_6, BEB cross sections are generally expected to be higher, not lower, than experimental values. In the experiment, SF_5 and SF_3 were generated by neutralizing the corresponding ions (at 2–3 keV in the laboratory frame). However, the authors of the experimental study excluded the possibility of internally excited target radicals, so we have no explanation why the measured values are so much higher than the BEB predictions at low energies.

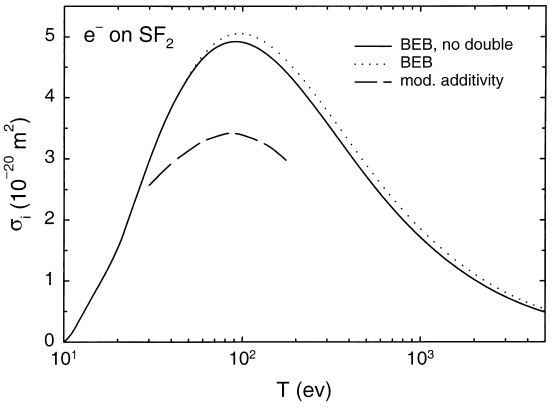

Fig. 5. Total ionization cross section for SF_2 under electron impact. The dashed curve shows the predictions from the modified additivity rule [7]. The solid and dotted curves are the predictions from BEB theory.

A value of 11.2 ± 1.0 eV for the ionization energy of SF_5 was obtained from the experimental data [7]. This agrees with our vertical value of 11.7 eV (Table 2) but is very different from recent adiabatic values of 9.71 ± 0.16 eV [8] and 9.52 eV [9], obtained from high-level ab initio calculations. This comparison supports our use of the vertical IE instead of adiabatic IE when computing BEB cross sections.

5.3. SF_3

The experimental peak is 3.5 ± 0.5 Å^2 at $T \approx 100$ eV. The BEB cross section is 5.1 Å^2 at $T = 121$ eV. This discrepancy is (49 ± 21)% in intensity and 21 eV in peak position. Only the SF_3^+ fragment was collected in the experiment. Other fragments such as SF_2^+, SF^+, S^+, and F^+ were estimated to contribute 0.2 Å^2 or less to the cross section [7]. Including them would shift the experimental peak to higher energy but can bring the discrepancy in intensity only as low as (40 ± 19)%. As for SF_5, the experimental cross sections at low T are, surprisingly, higher than the theoretical values.

An ionization energy of 11.0 ± 1.0 eV for SF_3 was extracted from the measured threshold [7]. This agrees with our vertical value of 11.1 eV (Table 2) but not with recent adiabatic values, from well-correlated

ab initio calculations, of 8.36 ± 0.18 eV [8] and 8.24 eV [9]. As for SF_5, this comparison supports our adoption of the vertical IEs when using BEB theory.

5.4. SF, SF_2, and SF_4

The BEB cross sections are displayed in Figs. 4, 5, and 6. No experimental results are available for comparison.

5.5. Comparison with the modified additivity rule

In the present article we restrict our attention to predictions for the radicals SF_x ($x = 1$–5), but note that several predictive methods have been reviewed very recently [37]. In addition to their experimental measurements, Tarnovsky et al. [7] used the empirical modified additivity rule (MAR) of Deutsch et al. [6] to calculate the total single ionization cross sections for all SF_x ($x = 1$–6). As shown in Figs. 2 and 3, the MAR cross sections agree better than the ab initio BEB cross sections with the experimental results for SF_5 and SF_3. Proponents of MAR will interpret this agreement as support for MAR, whereas proponents of BEB will interpret this comparison as revealing some experimental problems. This potential disagreement can only be resolved by further experiments. Nonetheless, it is still possible to make some useful, general comparisons between BEB and MAR.

Both BEB and MAR promise comparable uncertainties. As discussed above, the BEB cross section may exceed the ionization cross section due to neutral processes that can result from electron impact. We typically consider BEB predictions to be reliable to within about 15%. The MAR predictions require values for the absolute ionization cross sections of atoms. Since these are typically known to within 15% or 20% [7], the MAR predictions can only be reliable to the same degree. Thus, any molecule for which the BEB and MAR predictions differ by more than 40% or 50% may provide a good contest for the two methods. Among the SF_x species, MAR predicts a larger cross section for SF and a smaller cross section for SF_2, relative to the heavier SF_x, than does BEB. Both methods predict the cross section for SF to peak at lower energy than for the higher homologues.

The BEB method is more computationally demanding than the MAR method. BEB requires at least a low-level ab initio calculation on the molecule of interest, whereas MAR, in principle, requires only simple calculations. However, computational cost is less important now than in past years, since powerful computers have rendered simple ab initio calculations routine (i.e. minutes on a personal computer). Some degree of expertise is required to perform the calculations, but improved desktop software has drastically reduced this barrier. Using the MAR method is not computationally demanding, but requires that some parameters be read from a graph [7]. Furthermore, it requires smoothed atomic cross section data over a wide range in T, for which there is no convenient source. We encourage the publication of precise equations to make the MAR predictions more reproducible.

The MAR method involves many adjustable parameters, including scaling factors for atomic radii. Like any parameterized, empirical procedure, it is expected to perform well for interpolations among similar molecules, but unevenly for extrapolations to dissimilar systems. In contrast, although some of its refinements were developed semiempirically (see above), the BEB method does not contain empirical or adjustable parameters. As a result, it is expected to have a broad range of applicability and to perform consistently for widely different systems, as it has done so far.

Acknowledgement

This work at NIST was supported in part by the Electronics and Photonics Technology Office of the Advanced Technology Program of NIST.

References

[1] Proceedings of the VIII International Symposium on Gaseous Dielectrics, L.G. Christophorou, J.K. Olthoff (Eds.), Plenum, New York, 1998.

[2] D. Rapp, P. Englander-Golden, J. Chem. Phys. 43 (1965) 1464.
[3] T. Stanski, B. Adamczyk, Int. J. Mass Spectrom. Ion Processes 46 (1983) 31.
[4] D. Margreiter, G. Walder, H. Deutsch, H.U. Poll, C. Winkler, K. Stephan, T.D. Märk, Int. J. Mass Spectrom. Ion Processes 100 (1990) 143.
[5] W. Hwang, Y.-K. Kim, M.E. Rudd, J. Chem. Phys. 104 (1996) 2956.
[6] H. Deutsch, K. Becker, T.D. Märk, Int. J. Mass Spectrom. Ion Processes 167/168 (1997) 503.
[7] V. Tarnovsky, H. Deutsch, K.E. Martus, K. Becker, J. Chem. Phys. 109 (1998) 6596.
[8] K.K. Irikura, J. Chem. Phys. 102 (1995) 5357.
[9] C.W. Bauschlicher Jr., A. Ricca, J. Phys. Chem. A 102 (1998) 4722.
[10] N.F. Mott, Proc. R. Soc. London, Ser. A 126 (1930) 259.
[11] H. Bethe, Ann. Phys. (Leipzig) 5 (1930) 325.
[12] W.F. Miller, Ph.D. thesis, Purdue University, 1956, unpublished.
[13] L. Vriens, in Case Studies in Atomic Physics, E.W. McDaniel, M.R.C. Mcdowell, (Eds.), North Holland, Amsterdam, 1969, Vol. 1, p. 335.
[14] P. Khare, Planet. Space Sci. 17 (1969) 1257.
[15] Y.-K. Kim, Radiat. Res. 61 (1975) 21; 64 (1975) 205.
[16] D.K. Jain, S.P. Khare, J. Phys. B 9 (1976) 1429.
[17] D. Margreiter, H. Deutsch, M. Schmidt, T.D. Märk, Int. J. Mass. Spectrom. Ion Processes 100 (1990) 157.
[18] Y.-K. Kim, M.E. Rudd, Phys. Rev. A 50 (1994) 3954.
[19] Y.-K. Kim, W. Hwang, N.M. Weinberger, M.A. Ali, M.E. Rudd, J. Chem. Phys. 106 (1997) 1026.
[20] M.A. Ali, Y.-K. Kim, W. Whang, N.M. Weinberger, M.E. Rudd, J. Chem. Phys. 106 (1997) 9602.
[21] Y.-K. Kim, M.A. Ali, M.E. Rudd, J. Res. Natl. Inst. Stand. Technol. 102 (1997) 693.
[22] H. Nishimura, W.M. Huo, M.A. Ali, Y.-K. Kim, J. Chem. Phys. 110 (1999) 3811.
[23] W.M. Huo, Y.-K. Kim, Chem. Phys. Lett., 319 (2000) 576.
[24] Most of these molecular cross sections, updated references, and molecular constants included in Refs. 18–22 are available on a NIST website: http://physics.nist.gov/ionxsec.
[25] Certain commercial materials and equipment are identified in this article in order to specify procedures completely. In no case does such identification imply recommendation or endorsement by the National Institute of Standards and Technology, nor does it imply that the material or equipment identified is necessarily the best available for the purpose.
[26] M.W. Schmidt, K.K. Baldridge, J.A. Boatz, S.T. Elbert, M.S. Gordon, J.H. Jensen, S. Koseki, N. Matsunaga, K.A. Nguyen, S.J. Su, T.L. Windus, M. Dupuis, J.A. Montgomery, J. Comput. Chem. 14 (1993) 1347.
[27] J.A. Pople, M. Head-Gordon, K. Raghavachari, J. Chem. Phys. 87 (1987) 5968.
[28] K. Raghavachari, G.W. Trucks, J.A. Pople, M. Head-Gordon, Chem. Phys. Lett. 157 (1989) 479.
[29] T.H. Dunning Jr., J. Chem. Phys. 90 (1989) 1007.
[30] D.E. Woon, T.H. Dunning Jr., J. Chem. Phys. 98 (1993) 1358.
[31] A.D. Becke, J. Chem. Phys. 98 (1993) 5648.
[32] P.J. Stephens, F.J. Devlin, C.F. Chabalowski, M.J. Frisch, J. Phys. Chem. 98 (1994) 11623.
[33] J.F. Stanton, J. Gauss, J.D. Watts, W.J. Lauderdale, R.J. Bartlett, Int. J. Quantum Chem. S26 (1992) 879.
[34] ACES II, an ab initio program system authored by J.F. Stanton, J. Gauss, J.D. Watts, W.J. Lauderdale, R.J. Bartlett. The package also contains modified versions of the MOLECULE Gaussian integral program of J. Almlöf, P.R. Taylor, the ABACUS integral derivative program of T.U. Helgaker, H.J.A. Jense, P. Jorgensen, P.R. Taylor, and the PROPS property integral package of P.R. Taylor.
[35] M.J. Frisch, et al. GAUSSIAN 98, Gaussian, Inc., Pittsburgh, PA, 1998.
[36] Y.-K. Kim, M.E. Rudd, Comments At. Mol. Phys. 34 (1999) 309.
[37] H. Deutsch, K. Becker, S. Matt, T.D. Märk, Int. J. Mass Spectrom. 197 (2000) 37.